Taylor & Francis
Taylor & Francis Group

Science and Technology for the Built Environment

ISSN: 2374-4731 (Print) 2374-474X (Online) Journal homepage: http://www.tandfonline.com/loi/uhvc21

Updated generalized natural gas reciprocating engine part-load performance curves for cogeneration applications

Thomas Zakrzewski & Brent Stephens

To cite this article: Thomas Zakrzewski & Brent Stephens (2017): Updated generalized natural gas reciprocating engine part-load performance curves for cogeneration applications, Science and Technology for the Built Environment, DOI: 10.1080/23744731.2016.1274623

To link to this article: http://dx.doi.org/10.1080/23744731.2016.1274623

Science and Technology for the Built Environment (2017) **0**, 1–8

ISSN: 2374-4731 print / 2374-474X online
DOI: 10.1080/23744731.2016.1274623

Updated generalized natural gas reciprocating engine part-load performance curves for cogeneration applications

THOMAS ZAKRZEWSKI and BRENT STEPHENS*

Department of Civil, Architectural, and Environmental Engineering, Illinois Institute of Technology, 3201 S. Dearborn St., Chicago, IL 60616, USA

The efficiency of combined heat and power systems, which most commonly utilize natural gas reciprocating engines, is strongly influenced by the performance of generation sets at part-load conditions. However, there is currently a lack of comprehensive data on the part-load performance of generation sets, which can lead to model inaccuracies when evaluating combined heat and power systems early in the design phase. The current work reviews recent manufacturer reports and several industry publications to summarize the part-load thermal and electric performance of 67 natural gas spark ignition reciprocating engines from a wide variety of manufacturers and nominal capacity ranges that are commonly used in combined heat and power applications. Comparisons between linear and nonlinear performance curves for part-load heat-to-power ratios and electric heat rates demonstrated that, for most cases, nonlinear Power Law functions more accurately characterize performance above 50% part-load. The data were also used to develop a set of generalized nonlinear performance curves that extend below 50% part-load ratio that are intended for engineers to use in evaluating combined heat and power systems when more detailed performance data is not available.

Introduction

Combined heat and power (CHP) systems can increase onsite energy efficiency through the simultaneous production of electricity and thermal energy. While a variety of heat and power generation technologies and fuels are used in cogeneration systems, natural gas reciprocating engines are most prevalent in commercial building CHP applications (EPA 2015). Two fundamental parameters govern generation set efficiency: (1) the electric heat rate (EHR), and (2) the heat-to-power ratio (HPR; Spiewak 1987). The EHR is the ratio of fuel input per unit of electricity output. The HPR is the ratio of useful thermal output to the electric output power. Although knowledge of these parameters for generation sets across a wide range of part-load ratios is crucial for accurate CHP system design and analysis, there is currently a lack of comprehensive data on the part-load performance of generation sets (Bianchi et al. 2014). In the absence of better data, co-generation models often use linear approximations to account for the part-load performance of generation sets (Bianchi et al. 2014; Cho et al. 2009; Ghadimi et al. 2014; Han et al. 2014; Kong et al. 2009; Marshman et al. 2010; Milan et al. 2015; Savola and Keppo 2005).

Received October 13, 2016; accepted December 10, 2016
Thomas Zakrzewski, Student Member ASHRAE, is a PhD Candidate. **Brent Stephens, PhD,** Associate Member ASHRAE, is an Associate Professor.
*Corresponding author e-mail: brent@iit.edu
Color versions of one or more of the figures in the article can be found online at www.tandfonline.com/uhvc.

However, recent studies have shown that part-load EHRs and HPRs for most generation sets are typically nonlinear (ASHRAE 2016; Bhatt 2001; Bush 2010; Cho 2009; Hajabdollahi et al. 2015; Kazempoor et al. 2011; Sanaye et al. 2008; Santo 2012; Williams et al. 1998). Failing to account for the nonlinear part-load performance of generation sets can result in inaccurate predictions of CHP performance in system models (Ashok and Banerjee 2003; Milan et al. 2015). Further, when investigations have incorporated nonlinear part-load performance curves (e.g., Hajabdollahi et al. 2015; Sanaye et al. 2008; Santo 2012), they have typically relied on older, often outdated, generation set performance data such as those provided in the ASHRAE *HVAC Systems and Equipment* Handbook (ASHRAE 2016). Moreover, ASHRAE's foremost comprehensive resource on cogeneration system design, the *Combined Heat and Power Design Guide* (Sweetser et al. 2015), remains aligned with the same outdated generation set performance data. Failing to account for the part-load performance of newer generation sets can also lead to inaccurate estimates of CHP system performance, as the efficiency of natural gas reciprocating generation sets has improved dramatically in recent years and is expected to continue to improve with higher EHRs and HPRs (NREL and GRI 2003).

Therefore, the objectives of this work are to (1) compile existing part-load thermal and electric performance data for natural gas type reciprocating engines used in CHP applications; (2) compare the accuracy of linear and nonlinear performance curves for representing their part-load performance; and (3) develop a set of updated generalized nonlinear performance curves for others to use in evaluating CHP systems. This work is intended to bridge the part-load

Table 1. Full generation set part-load performance data (down to 50% part-load).

Generation set manufacturer	Model	Rated power capacity (kW)	Heat-to-power ratio (kW/kW) Generation set part-load power rating 50%	75%	90%	100%	Electric heat rate (Btu/kWh) Generation set part-load power rating 50%	75%	90%	100%
ISI		35				2.17				11,743
PEI		43				1.91				12,791
Tecogen		60				2.15				12,667
ISI		60				2.47				12,917
Tecogen	CM-S60	60				2.24				13,033
Tecogen	CM-U60	60				2.14				13,033
PEI		72				1.90				11,278
Tecogen		75				1.84				11,507
Tecogen	CM-S75	75				2.00				12,360
Tecogen	CM-U75	75				1.91				12,360
MCC		85				1.32				6694
PEI		100				1.91				10,930
Tecogen	INV-S100	100	2.27	2.06	2.03	2.05	12,894	12,372	12,495	12,628
Tecogen	INV-U100	100				1.96				12,380
EPA 2008[2]	System-1	100				1.79				12,000
EPA 2015[3]	System-1	100				1.96				12,637
EPA 2007[1]	System-1	100				1.64				11,500
ISI		120				1.37				8742
MTU	GC 128	128				0.60				10,023
Caterpillar	G3406 NA	172	2.28	1.91		1.64	310,865	181,783		123,916
MTU	GC 248	248				0.59				10,060
Caterpillar	G3406	250	1.92	1.69		1.55	181,283	113,063		80,438
EPA 2008[2]	System-2	300				1.27				9866
EPA 2007[1]	System-2	300				1.49				11,000
Caterpillar	G3412 TA	350	2.73	2.09		1.77	155,595	86,309		58,128
MTU	GC 358	358				2.00				9349
Caterpillar	G3412C	375	2.44	1.77		1.48	143,709	79,265		52,424
Caterpillar	G3512	555	2.31	1.99		1.81	90,577	55,556		39,457
Caterpillar	G3512	570	1.82	1.55		1.43	80,267	49,882		36,385
Caterpillar	G3512	585	1.79	1.53		1.41	78,343	48,629		35,452
EPA 2015[3]	System-2	633				1.28				9896
Caterpillar	G3516 TA	740	2.02	1.76		1.62	65,656	39,901		28,431
MTU	MTU 8V4000	762				1.86				8295
EPA 2008[2]	System 3	800				1.27				9760
Caterpillar	G3516 LE	820	1.52	1.39		1.15	53,391	34,251		24,063

Cummins	C1000 N6C	1000	0.84	0.63	0.61	0.64	28,974	19,316	16,097	14,487
Cummins	C1000 N6C	1000	0.67	0.64	0.60	0.63	28,974	19,316	16,097	14,487
EPA 2007[1]	System 3	1000				1.09				10,200
GE	JMS 320 GS-N.L.	1059				1.30				17,075
Cummins	C1100 N6C	1100	0.77	0.65	0.64	0.63	26,340	17,560	14,633	13,170
EPA 2015[3]	System-3	1121				1.12				9264
MTU	MTU 12V4000	1151				1.70				8917
Cummins	1250 N6C	1250		1.00	0.92	0.89		15,453	12,877	11,590
Cummins	C1400 N6C	1400	1.10	0.97	0.95	0.93	20,696	13,797	11,498	10,348
Cummins	C1400 N6C	1400	1.12	0.98	0.95	0.93	20,696	13,797	11,498	10,348
GE	JMS 420 GS-N.L.	1426				1.11				15,732
Caterpillar	G3516B LE	1470	1.87	1.20		1.12	40,742	19,014		13,672
Caterpillar	G3516B LE	1470	1.34	1.18		1.08	29,832	18,595		13,297
MTU	G3520C	1600	1.22	0.99		0.84	25,123	15,658		11,317
Caterpillar	G3520C	1600	1.44	1.19		1.06	25,267	15,757		11,391
Caterpillar	G3516C	1660	1.26	1.11		0.96	24,417	15,514		11,230
Caterpillar	MTU 16V4000	1697				1.69				8114
Cummins	C1750 N6C	1750	0.93	0.80	0.77	0.77	16,557	11,038	9,198	8278
Caterpillar	G3520C	1900	1.41	1.20		1.09	22,135	13,809		10,111
Caterpillar	G3520C	1900	1.45	1.23		1.11	22,686	14,155		10,363
MTU	C2000 N6C	2000	1.00	0.85	0.82	0.80	14,487	9,658	8,048	7244
Cummins	G3520C	2055	1.38	1.20		1.04	20,661	13,086		9431
Caterpillar	G3520C	2055	1.35	1.18		1.03	20,132	12,754		9194
Caterpillar	MTU 20V4000	2129				1.79				8078
EPA 2008[2]	System-4	3000				1.03				9492
EPA 2007[1]	System-4	3000				0.96				9533
Caterpillar	G3616	3105	1.08	0.94		0.81	12,115	7,769		5675
GE	JMS 620 GS-N.L.	3326				0.97				4791
EPA 2015[3]	System-4	3326				0.94				8454
EPA 2008[2]	System-5	5000				0.89				8758
EPA 2007[1]	System-5	5000				0.98				9213
EPA 2015[3]	System-5	9341				0.84				8207

Note: Biomass combined heat and power catalog of technologies—U.S. environmental protection agency combined heat and power partnership (September 2007).
Technology characterization: reciprocating engines—U.S. environmental protection agency combined heat and power partnership (December 2008).
Catalog of CHP technologies—U.S. environmental protection agency combined heat and power partnership (March 2015).

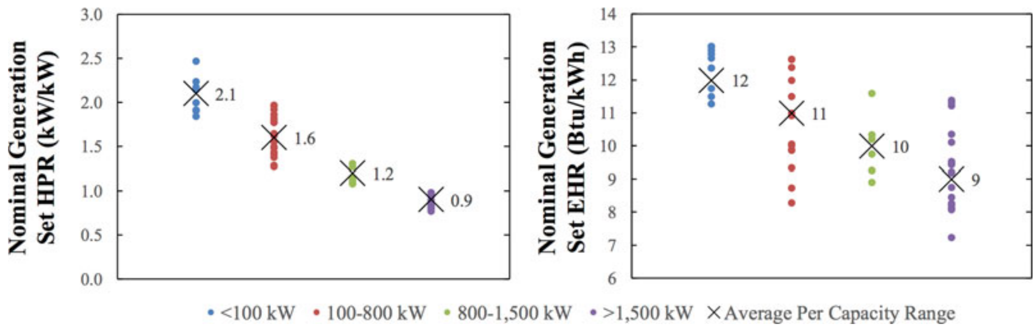

Fig. 1. Nominal generation set capacity ranges and arithmetic means in each size range for a: heat-to-power ratio (**HPR**); and b: electric heat rate (**EHR**).

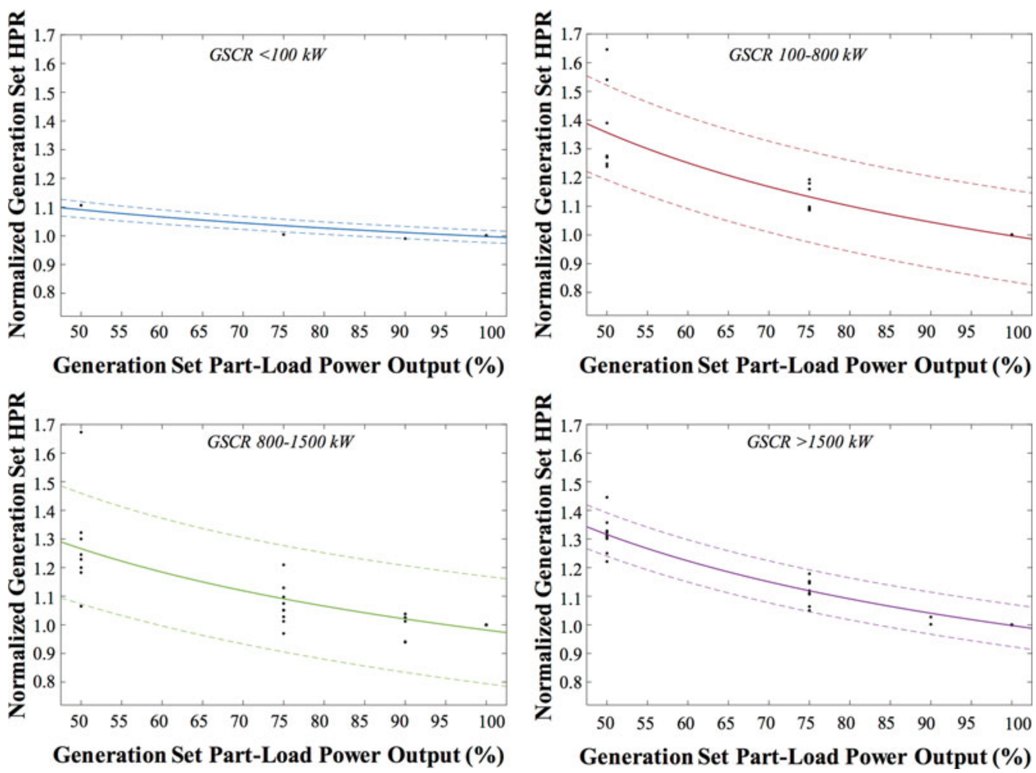

Fig. 2. Non-linear (Power Law) part-load regression fits for normalized heat-to-power ratios (**HPR**) for four distinct generation set capacity ranges (**GSCR**). Data are limited to 50%–100% part-load ratios from Table 1.

Table 2. Linear regression results for normalized part-load generation set performance.

				$f(x) = \text{p1} \times x + \text{p2}$		95% Confidence bounds	
Generation set parameter	Fit type	Capacity range	R^2	p1	p2	p1	p2
Electric heat rate	Linear	<100 kW	0.086	– 0.0001693	1.016	(−0.0004433, 0.0001046)	(0.9893, 1.042)
Electric heat rate	Linear	100–800 kW	0.930	– 0.02695	3.648	(−0.02966, –0.02424)	(3.419, 3.877)
Electric heat rate	Linear	800–1500 kW	0.862	– 0.02316	3.244	(−0.02621, –0.02011)	(2.987, 3.5)
Electric heat rate	Linear	>1500 kw	0.923	– 0.02204	3.15	(−0.02411, –0.01997)	(2.978, 3.321)
Heat-to-power ratio	Linear	<100 kW	0.768	– 0.001707	1.168	(−0.002172, –0.001243)	(1.124, 1.213)
Heat-to-power ratio	Linear	100–800 kW	0.775	– 0.006979	1.688	(−0.008357, –0.005602)	(1.572, 1.804)
Heat-to-power ratio	Linear	800–1500 kW	0.566	– 0.005465	1.522	(−0.007107, –0.003823)	(1.384, 1.659)
Heat-to-power ratio	Linear	>1500 kW	0.917	– 0.00624	1.614	(−0.006858, –0.005622)	(1.563, 1.666)

Table 3. Non-linear (Power Law) regression results for normalized part-load generation set performance.

				$f(x) = a \times x$^b		95% Confidence bounds	
Generation set parameter	Fit type	Capacity range	R^2	a	b	a	b
Electric heat rate	Power	<100 kW	0.138	1.075	– 0.01599	(0.9787, 1.171)	(– 0.03567, 0.003683)
Electric heat rate	Power	100–800 kW	0.969	339.8	– 1.266	(222.2, 457.3)	(– 1.35, –1.183)
Electric heat rate	Power	800–1,500 kW	0.904	185.6	– 1.137	(95.25, 275.9)	(– 1.252, –1.021)
Electric heat rate	Power	>1,500 kw	0.978	172.3	– 1.122	(133.5, 211.1)	(– 1.176, –1.068)
Heat-to-power ratio	Power	<100 kW	0.841	1.804	– 0.1286	(1.586, 2.023)	(– 0.1553, –0.102)
Heat-to-power ratio	Power	100–800 kW	0.795	7.716	– 0.4444	(5.056, 10.38)	(– 0.5245, –0.3642)
Heat-to-power ratio	Power	800–1500 kW	0.301	5.318	– 0.3668	(3.043, 7.592)	(– 0.4658, –0.2679)
Heat-to-power ratio	Power	>1500 kW	0.933	6.265	– 0.3989	(5.34, 7.189)	(– 0.4332, –0.3647)

performance gap between technical data from manufacturers and industry publications to better inform generation set design sizing and operational mode selection.

Data collection and analysis

Performance data for various makes and models of lean burn natural gas spark ignition reciprocating engines from manufacturer reports and several industry publications were reviewed to assess the relationship between part-load capacity of generation set coincident to fuel consumption, net electricity generation, and useful recovered heat. Most of the performance data were culled from manufacturer reports, which rate engine capacities according to *ISO Standard 3046–1 Reciprocating Internal Combustion Engine Performance*. ISO 3046–1 uses standard reference conditions to quantify the performance and availability for continuous and part-load operation, typically between 50% and 100% of nominal capacity (International Organization for Standardization 2002). Data from natural gas type spark ignition reciprocating engines with rated capacities ranging from 35 kW to 10 MW were screened as the typical range of commercially available generation sets for a wide range of CHP applications ranging from individual buildings to entire campuses of mixed building typologies.

The electrical output power, HPR, and EHR performance characteristics were selected as essential parameters to define CHP performance over a range of loads. Both linear and nonlinear regressions were applied to the resulting part-load performance data using the Curve Fitting Toolbox™ in

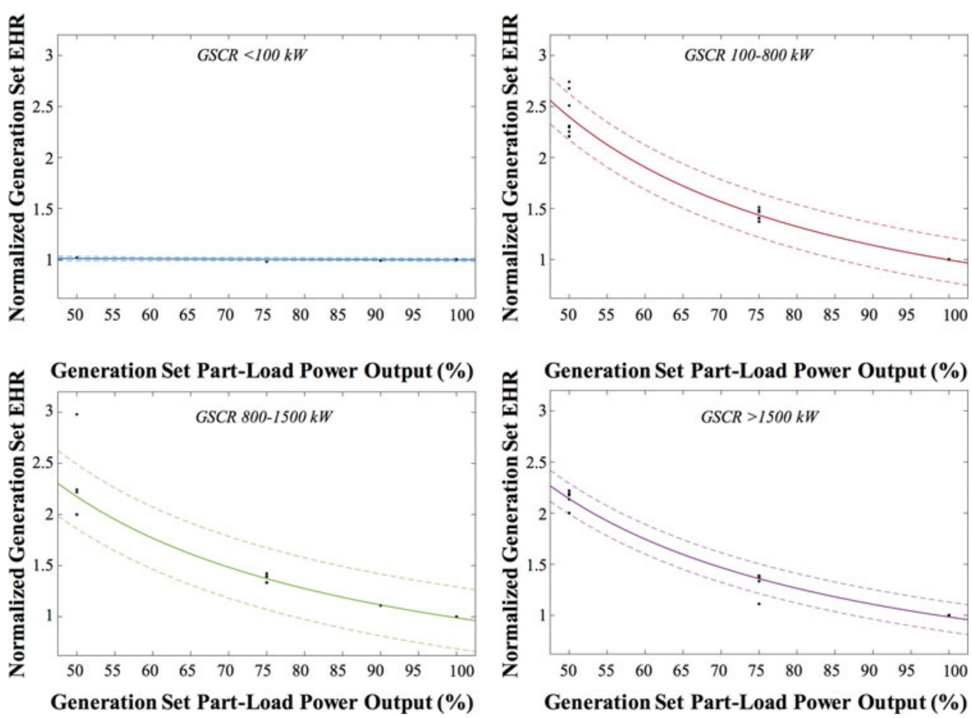

Fig. 3. Non-linear (Power Law) part-load regression fits for normalized electric heat rate (**EHR**) for four distinct generation set capacity ranges (**GSCR**). Data are limited to 50%–100% part-load ratios from Table 1.

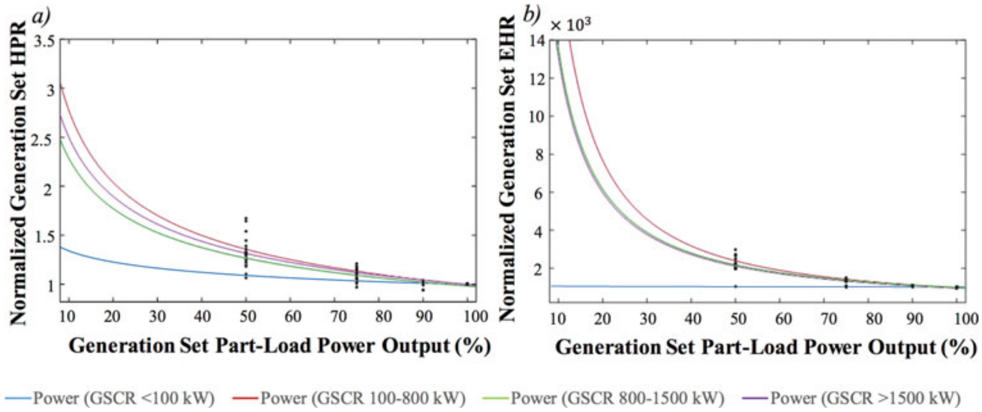

Fig. 4. Performance curves normalized by generation set capacity range (**GSCR**): a: heat-to-power ratio (**HPR**) and b: electric heat rate (**EHR**). Performance curve projections are extended to 10% of the full-load generation set output rating.

MATLAB (MathWorks R2015a). Regressions were first fit only for part-load ratios ranging from 50% to 100%. Coefficients of determination (R^2) were used to evaluate regression fit and 95% confidence intervals were used to assess model uncertainty. Then backward regression forecasting was applied to estimate performance below 50% of the generation set full-load power output for which there were no manufacturer-reported data.

Next, while it is understood that performance is unique to the specific make and model of a generation set, general performance characteristics aggregated over a large amount of performance data can also be used for more generalized analyses. Therefore, the resulting data set was also used to develop generalized performance curves that reasonably represent the part-load dependence of the HPR and EHR for the range of natural gas reciprocating generation sets identified herein. In generalizing these data, the authors purposefully focused on data above 50% part-load to reflect knowledge from available ISO 3046–1 performance data (for which the authors have more confidence), but also project below 50% part-load to demonstrate the potential uncertainty introduced by limiting part-load performance data to 50% and above (for which the authors have less confidence).

Results and discussion

Generation set performance data were obtained for a total of 67 natural gas spark ignition reciprocating engines from a wide variety of manufacturers (Table 1). The natural gas type reciprocating engines are representative of published nominal and part-load performance data available since 2007. Generally, as the nominal electric power generation capacity of a generation set increases, both the HPR and EHR decrease. Therefore, the generation sets in Table 1 were divided into four distinct nominal generation set capacity ranges (GSCRs): <100 kW, 100–800 kW, 800–1500 kW, and >1500 kW (Figure 1). These four GSCRs were found by iteratively grouping the generation set performance data by nominal output power until there were no significant linear correlations between the HPR and the nominal electric generation capacity in each bin (i.e., $R^2 < 0.1$). These GSCRs are in general agreement with similar efforts to generalize reciprocating engine prime movers for cogeneration screening analysis (Orlando 1996).

Figures 2 and 3 show nonlinear (Power Law) curve fits through the resulting 50%–100% part-load HPR and EHR data, respectively, for each of the four defined GSCRs.

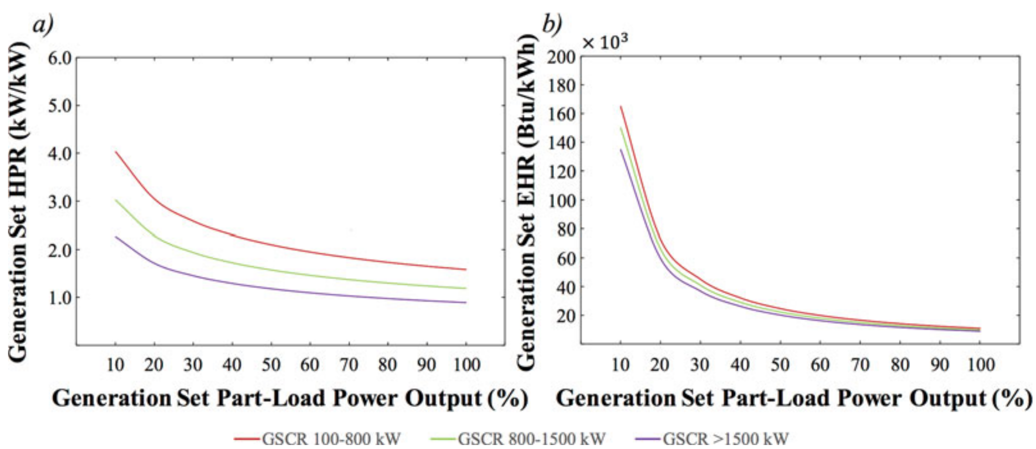

Fig. 5. Proposed generalized generation set part-load performance curves for cogeneration applications: a: heat-to-power ratio (HPR) and b: electric heat rate (EHR).

Table 4. Proposed generalized generation set part-load performance functions and capacity coefficients for heat-to-power ratio and electric heat rate.

			$f(x) = c \times a \times x^\wedge b$		
Generation set parameter	Fit type	Capacity range	a	b	C
Electric heat rate	Power	100–800 kW	227.9	−1.182	11,000
Electric heat rate	Power	800–1500 kW	227.9	−1.182	10,000
Electric heat rate	Power	>1500 kw	227.9	−1.182	9000
Heat-to-power ratio	Power	100–800 kW	6.399	−0.4048	1.60
Heat-to-power ratio	Power	800–1500 kW	6.399	−0.4048	1.20
Heat-to-power ratio	Power	>1500 kW	6.399	−0.4048	0.90

Dashed lines represent 95% confidence intervals based on the regression outputs. The HPR and EHR data are normalized by the nominal output capacity of each unit. Only nonlinear curve fits are shown because they generally resulted in better fits than linear regressions (see Tables 2 and 3).

Figure 4 shows these same Power Law curve fits applied to the four ranges of GSCRs for both normalized HPR and EHR, extended below 50% part-load ratio. With the exception of generation sets with rated power capacities below 100 kW, the curve fits in Figure 4 support the use of a characteristic long-tailed power distribution at part-load, which is consistent with ASHRAE and other references (e.g., Bush 2010; Cho 2009). While the extrapolations below 50% part-load ratio in Figure 4 must be interpreted with considerable uncertainty, they align reasonably well with the very limited data on sub-50% part-load ratio performance from other studies (ASHRAE 2016; Bhatt 2001; Bush 2010; Williams et al. 1998).

Given the similarity of the curve fits for all GSCRs above 100 kW, Figure 5 shows proposed generalized part-load Power Law performance functions for natural gas generation sets above 100 kW nominal capacity. Table 4 summarizes the same proposed generalized performance functions and capacity coefficients for both HPR and EHR. The derived capacity coefficients are applied to the Power Law expression as a constant, *c*, to account for the nominal generation set output power displacement. These generalized curves can be used to characterize part-load performance of generation sets above 100 kW in nominal capacity with reasonable accuracy when more detailed information is not available.

Conclusion

This work demonstrates that nonlinear power-law regressions for both the HPR and EHR of a large number of natural gas reciprocating engines available for use in CHP applications are typically more accurate than a linear assumption, even with limited part-load performance data and high uncertainty below 50% of the nominal power output. Given some of the data limitations demonstrated here and the importance of accurately characterizing part-load performance for CHP applications, more research should focus on understanding the sensitivity of part-load performance of generation sets below 50% and above minimum turn-down constraints. Until then, the proposed generalized part-load performance curves can be used to improve decision making and accuracy early in the design phase when detailed or specific performance data are limited or not available.

Funding

This work was partially supported by the 2016 William (Bill) Mashburn Scholarship awarded by the Foundation of the Association of Energy Engineers (FAEE).

References

Ashok, S., and R. Banerjee. 2003. Optimal operation of industrial cogeneration for load management. *IEEE Transactions on Power Systems* 18(2):931–7.

ASHRAE. 2016. *Combined Heat and Power Systems. ASHRAE Handbook—HVAC Systems and Equipment, by Cogeneration Systems ASHRAE TC 1.10*. Atlanta: ASHRAE.

Bhatt, M.S. 2001. Mapping of general combined heat and power systems. *Energy Conversion and Management* 42:115–24.

Bianchi, M., A. De Pascale, F. Melino, and A. Peretto. 2014. Performance prediction of micro-CHP systems using simple virtual operating cycles. *Applied Thermal Engineering* 71:771–9.

Bush, J. 2010. Modeling of a combined heat and power unit and evaluation of system performance in building applications. Thesis, Mechanical Engineering, University of College Park, Maryland, USA; ProQuest/UMI Number: 1478119.

Cho, H.J. 2009. Dynamic simulation and optimal real-time operation of CHP systems for buildings. Dissertation, Mechanical Engineering, Mississippi State University, Mississippi, USA; ProQuest/UMI Number: 3352267.

Cho, H.J., P.J. Mago, R. Luck, and L.M. Chamra. 2009. Evaluation of CCHP systems performance based on operational cost, primary energy consumption, and carbon dioxide emission by utilizing an optimal operation scheme. *Applied Energy* 86:2540–9.

Ghadimi, P., S. Kara, and B. Kornfeld. 2014. The optimal selection of on-site CHP systems through integrated sizing and operational strategy. *Applied Energy* 126:38–46.

Hajabdollahi, H., A. Ganjehkaviri, M. Jaafar, and M. Nazri. 2015. Assessment of new operational strategy in optimization of CCHP plant for different climates using evolutionary algorithms. *Applied Thermal Engineering* 75(22):468–80.

Han, G., S. You, T. Ye, P. Sun, and H. Zhang. 2014. Analysis of combined cooling, heating, and power systems under a compromised electric-thermal load strategy. *Energy and Buildings* 84:586–94.

International Organization for Standardization (ISO). 2002. ISO 3046–1:2002 Reciprocating internal combustion engines—Performance Part 1: Declarations of power, fuel and lubricating oil consumptions, and test methods—Additional requirements for engines for general use. Geneva, Switzerland: ISO.

Kazempoor, P., V. Dorer, and A. Weber. 2011. Modelling and evaluation of building integrated SOFC systems. *International Journal of Hydrogen Energy* 36:13241–9.

Kong, X.Q., R.Z. Wang, Y. Li, and X.H. Huang. 2009. Optimal operation of a micro-combined cooling, heating and power system driven by a gas engine. *Energy Conversion and Management* 50:530–8.

Marshman, D.J., T. Chmelyk, M.S. Sidhu, R.B. Gopaluni, and G.A. Dumont. 2010. Energy optimization in a pulp and paper mill cogeneration facility. *Applied Energy* 87:3514–25.

MathWorks. 2015a. "MATLAB." Natick. http://www.mathworks.com/products/matlab/.

Milan, C., M. Stadler, G. Cardoso, and S. Mashayekh. 2015. Modeling of non-linear CHP efficiency curves in distributed energy systems. *Applied Energy* 148:334–47.

National Renewable Energy Laboratory (NREL) and Gas Research Institute (GRI). 2003. *Gas-Fired Distributed Energy Resource Technology Characterizations*. Washington, DC: U.S. Department of Energy—Energy Efficiency and Renewable Energy.

Orlando, J.A. 1996. *Cogeneration Design Guide*. Atlanta: ASHRAE.

Sanaye, S., M.A. Meybodi, and S. Shokrollahi. 2008. Selecting the prime movers and nominal powers in combined heat and power systems. *Applied Thermal Engineering* 28:1177–88.

Santo, E.D.B. 2012. Energy and exergy efficiency of a building internal combustion engine trigeneration system under two different operational strategies. *Energy and Buildings* 53: 28–38.

Savola, T., and I. Keppo. 2005. Off-design simulation and mathematical modeling of small-scale CHP plants at part loads. *Applied Thermal Engineering* 25:1219–32.

Spiewak, S.A. 1987. *Cogeneration and Small Power Production Manual*. Lilburn, GA: The Fairmont Press, Inc.

Sweetser, R., G. Foley, J. Freihaut, B. Hedman, L. Hyman, D. Paraschiv, G. Bares, and T. Wagner. 2015. *Combined Heat and Power Design Guide*. Atlanta: ASHRAE.

U.S. Environmental Protection Agency (EPA) and Combined Heat and Power Partnership. 2015. *Catalog of CHP Technologies*. Washington, DC: U.S. Environmental Protection Agency.

Williams, J.M., A.J. Griffiths, and I.P. Knight. 1998. Knowledge-based sizing of cogeneration plant in buildings. *ASHRAE Transactions* 104:24–31.